PHYSICAL REVIEW B **80**, 220102(R) (2009)

Interstitials in tetrahedrally close-packed phases: C, N, O, and F in β-tungsten from first principles

Marcel H. F. Sluiter[*]
Department of Materials Science & Engineering, Delft University of Technology, Mekelweg 2, 2628CD Delft, The Netherlands

(Received 24 August 2009; published 9 December 2009)

Several tetrahedrally close-packed (tcp) phases, such as β-W, β-Ta, and β-U, are believed to be stabilized by impurities. Here we analyze the various ways in which impurities can be dissolved in tcp structures paying special attention to interstitial configurations in the β-W (A15) structure. We find that at most there are only seven interstitial positions possible. Through *ab initio* calculations we show that common impurities such as C, N, O, and F, dissolve interstitially in β-W and that N, O, and F interstitials prefer the same position in the β-W (A15) structure.

DOI: 10.1103/PhysRevB.80.220102 PACS number(s): 64.60.Bd, 61.72.jj, 61.66.Bi, 68.55.−a

Impurities are known to strongly affect structural stability and phase stability. A particular example is W, known to be body-centered cubic (bcc) when pure,[1] but taking the β-W, A15 (Strukturbericht notation), Cr_3Si prototype structure when impurities are present.[2,3] Other early transition metals, such as Cr, Mo, and Nb also, are known to occur with the β-W crystal structure[4–13] and recent *ab initio* calculations show tetrahedrally close-packed (tcp) structures for several elements to be only just above the ground-state structures[14,15] For some impurities there is (x-ray) evidence that they are substitutionally dissolved. For the lighter elements, such as C, N, O, and F, x-ray intensities are too weak to determine whether these impurities are of a substitutional or an interstitial nature. Here we seek to address this question by first analyzing the interstitial positions in tcp phases in general, and then applying our analysis to the Cr_3Si prototype structure. This reveals that there are just seven interstitial positions available in addition to the two substitutional positions.

Tcp structures have as a characteristic that tetrahedra formed between nearest neighbors (nn's) are space filling. These nn tetrahedra can share a vertex (atomic site), an edge (nn pair), or a facet (triangle formed between three nn pairs), but they never overlap. It follows that the largest interstices are centered within the tetrahedra, or possibly, are located at the centers of facets (triangles) where two tetrahedra are joined, i.e., at the centers of triangular-base bipyramids. Other positions, such as the mid point between edges, are less likely because of large strains. Having identified the possible interstitial sites with centers of nn tetrahedra and nn triangles, it remains to find the relevant tetrahedra and triangles. This has been done routinely in cluster-variation studies of complex phases.[16–19] The FeCr-prototype σ structure consists of 17 nn tetrahedra and 29 nn triangles, making for a total of 46 possible interstitial positions; and the Fe_7W_6-prototype μ structure consists of 13 nn tetrahedra and 20 nn triangles, making for a total of 33 possible interstitial positions. In simple lattices such as bcc and fcc there are just two interstitial positions (tetrahedral and octahedral). Clearly, interstitials in tcp phases are much more complex. Fortunately, the Cr_3Si-prototype A15 case is quite transparent still: The Cr_3Si-prototype structure, space group #223, see Fig. 1, has Si-type positions (small green spheres), with Wyckoff designation 2a, at the cube corners and at the body center, and has pairs of Cr-type positions (large red spheres) on the face centers at the Wyckoff 6c positions. Thus, there are two kinds of substitutional single-site defects: those on the Si positions, and those on the Cr positions. The three types of nn pairs are easily recognized in Fig. 1: the P1 nn pair occurs between Cr-type sites, such as between sites 1 and 2; P2 is between Cr- and Si-type sites, such as between 2 and 5; and P3 occurs between Cr sites such as 1 and 3. There are four types of nn triangles: Tr1 between sites 3,4,5; Tr2 sites 1,2,3; Tr3 sites 2,3,5; and Tr4 sites 2,4,6. Tr4, an equilateral triangle involving three P3s, is largest, and Tr1 and Tr2 are smallest. There are just three types of nn tetrahedra: Th1 between atoms 2,4,5,6 (involving three Tr3 and 1 Tr4); Th2 between atoms 2,3,4,5 (one Tr1, one Tr2, and two Tr3); and Th3 between atoms 1,2,3,4 (four Tr2). Th2 and Th3 have the same volume; Th1 is 12.5% larger. With these details, we can now understand that relaxation of an interstitial in a tetrahedron can cause it to move to a triangular face and vice versa. Thus the central point in Th1 can relax toward the center of Tr3 or Tr4 but not to Tr1 or to Tr2. Likewise Th2 may relax toward Tr1, Tr2, or Tr3, and Th3 may relax toward Tr2 only. So while geometry indicates there are possibly three tetrahedral and four triangular bipyramidal interstices, these seven positions can be realized only if the potential-energy surface

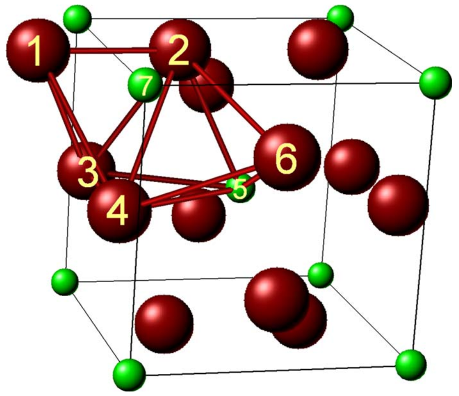

FIG. 1. (Color online) The cubic Cr_3Si prototype cell, Cr(Si) positions indicated as large red (small green) spheres. The 7 possible interstices positions are: Th1) center of sites 2,4,5,6; Th2) 2,3,4,5; Th3) 1,2,3,4; Tr1) 3,4,5; Tr2) 1,2,3; Tr3) 2,3,5; and Tr4) 2,4,6.

TABLE I. Excess properties of oxygen in tungsten.

α,p	$H^{\alpha,p}$ eV/cell	$\Delta H_{xs}^{\alpha,p}$ eV/O	$V^{\alpha,p}$ Å^3/cell	$\Delta V_{xs}^{\alpha,p}$ Å^3/O
bcc W_{54}	−697.718		865.00	
bcc $W_{54}O^{(o)}$	−701.760	−4.042	873.35	8.35
bcc $W_{54}O^{(t)}$	−702.071	−4.353	874.39	9.39
A15 W_{64}	−821.597		1038.84	
A15 $W_{63}O^{(Si)}$	−809.667	−0.908	1032.92	10.31
A15 $W_{63}O^{(Cr)}$	−810.331	−1.571	1032.76	10.15
A15 $W_{48}O_{16}^{(Si)}$	−649.291	−2.068	913.76	8.41
A15 $W_{64}O^{(Th2)}$	−826.307	−4.709	1048.01	9.17
A15 $W_{64}O^{(Th3)}$	−825.548[a]	−3.950[a]	1047.89[a]	9.05[a]
A15 $W_{64}O^{(Tr1)}$	−824.960[a]	−3.363[a]	1050.59[a]	11.75[a]
A15 $W_{64}O^{(Tr4)}$	−827.078	−5.481	1045.42	6.58

[a] Th3 and Tr1 are saddle-point configurations.

has local minima there. Moreover, it is evident that interstitial diffusion in tcp structures also, must be analyzed in terms of nn tetrahedra and nn triangles.

There is an extensive literature on the many impurities that can stabilize β-W, such as oxygen,[20,21] nitrogen,[20] carbon,[22,23] fluorine,[24] silicon,[25] or germanium.[26] Si is known to occupy the Si-type sites, in analogy with the Cr_3Si prototype, and the same is to be expected for Ge. The way oxygen is dissolved remains unclear. Currently deemed most probable are: substitutional, but without preference for either the Cr type of the Si-type sites,[3,20] interstitial,[20,21] or at grain boundaries and other defects.[27,28] Here, I will compute the relative stability of dilute solutions of substitutional and interstitial type as well as the case where O occupies all Si-type sites, giving W_3O. For purpose of comparison, O is considered as tetrahedral (t) and octahedral (o) interstitial in bcc W also.

Enthalpies (total energies) have been computed within the local-density approximation[29] using the Vienna *ab initio* simulation program (VASP) (Refs. 30 and 31) at a pressure of 0 GPa. The calculations were performed using pseudopotentials of the projector augmented wave (PAW) type.[32,33] The standard potentials were used for W, C, N, O, and F, which treat the 6s and 5d, and the 2s and 2p such as states as valence electrons. Integrations in reciprocal space use a Γ-centered $4\times4\times4$ Monkhorst-Pack[34] grid in the 1^{st} Brillouin zone pertaining to the 64-atom $2\times2\times2$ A15 cell. Precision was set to "accurate." In all calculations, the electronic wave functions were expanded in terms of plane waves up to a cutoff kinetic energy of 400 eV. The Hermite-Gauss smearing method of Methfessel and Paxton[35] of order 1 has been used, with a smearing parameter of 0.1 eV. The convergence criteria for energy and force were 0.1 meV and 10 meV/nm, respectively. Structural optimizations were reinitiated at least twice. For final static calculations real-space projectors were turned off and the linear tetrahedron method with Blöchl corrections[36] was used for the reciprocal space integrations. Calculations pertaining to bcc used a 54-atom cell consisting of $3\times3\times3$ bcc cubes with a Γ-centered $5\times5\times5$ Monkhorst-Pack[34] k-point grid.

The energetic stability of solute X at position "p" in structure α was considered by defining an excess enthalpy per X atom,

$$\Delta H_{xs}^{\alpha,p} = \frac{1}{m}\left[H^{\alpha}(W_k X_m^p) - \frac{k}{n}H^{\alpha}(W_n)\right]. \tag{1}$$

When "p" is an interstitial (substitutional) position $k=n$ ($k+m=n$). Similarly, excess volumes can be defined. The excess volume per X atom in position "p" can be expressed as

$$\Delta V_{xs}^{\alpha,p} = \frac{1}{m}\left[V^{\alpha}(W_k X_m^p) - \frac{k}{n}V^{\alpha}(W_n)\right]. \tag{2}$$

The enthalpies computed for various structures with and without oxygen are listed in Table I. It is apparent that oxygen prefers the tetrahedral interstice in bcc W because its excess enthalpy is lower. The enthalpy difference suggests that normally all oxygen in bcc W is in the (t) rather than (o) position. For the A15 structure three interstitial positions appear to be missing: Th1 position relaxes toward Tr4, and both Tr2 and Tr3 relax toward Th2. Local minima in the potential energy exist for Th2 and Tr4 only. Th3 and Tr1 are saddle-point configurations with two positive curvatures and one negative curvature. Interstitial position Tr4 is much more stable than the Th2 position, or the two saddle points, the excess enthalpy shows. It is apparent that O cannot dissolve substitutionally; the Cr position and both the single and complete substitution of the Si positions are several eV above the interstitial positions. This is hardly surprising as O is much too small an atom to replace W. The large differences among interstitial positions deserve some attention. It is tempting to explain the Tr4 preference because of the good fit of this interstice to the O atom, as appears from the small excess volume. However, this is an oversimplification as a comparison of (t) and (o) in bcc reveals. The (t) interstice requires, on average, less relaxation of surrounding W atoms to accommodate the oxygen atom than the (o) interstice: the W-O distance increases by 11% for all 4 bonds for (t), for (o) there are two short bonds that get stretched by 22% upon relaxation, and four longer bonds that are stretched just 2%. The elastic energy is roughly proportional to the square of the elongation. The (o) elastic energy is then proportional to 2×0.22^2 versus 4×0.11^2 for (t), assuming similar bond stiffness. In the (o) position, oxygen is inserted in the middle of a strong W-W bond (second nn), constricting outward relaxation and giving a rather small excess volume in spite of the high local elastic energy. A similar reasoning explains the stability of the Tr4 position: it is the largest triangle and it is equilateral, and the joint of the largest tetrahedra, forming a symmetric bipyramid. After relaxation all five nn's have equal W-O distances, making for an optimal dispersion of strain. In contrast, the Th2 and Th3 positions involve cages with 1 and 2 of the shortest W-W distances, and the same holds for the narrow isosceles triangle Tr1. Hence, the topological details matter. The excess enthalpy indicates that O normally occupies only the Tr4 position in A15. The excess enthalpy of O in A15 is more favorable than in bcc. This is in line with the lesser strained five equally spaced W-O bonds in A15 as opposed the four equal-spaced bonds in bcc. Bipyramids formed between nn's are not available in the bcc structure. The (o) position might be regarded as a square bipyramid, but with flattened pyramids that are not spacious. As A15 has a more than 1 eV advantage over bcc for every dissolved O atom, barring strong-interaction effects, a concentration of just over $7^{a}/_{o}$ O in W is sufficient to make bcc and A15 energetically degenerate.[37] In the literature both higher and lower O concentrations have been reported for stabilizing β-W: from 14 to 19 atomic percent ($^{a}/_{o}$),[38] $6-10^{a}/_{o}$,[21] $1-4^{a}/_{o}$,[39] 5–12,[28,40] $14-16^{a}/_{o}$.[27]

It is of interest if C, N, and F behave similar to O. The smaller C and N atoms prefer the (o) interstice in bcc W, while O and F take the (t) interstice (see Table II). In the A15 structure the Th1, Tr2, and Tr3 positions are unstable for C, N, and F just as for O. All four solutes appear to take the Tr4 position, but in fact C deviates. C fits into an irregular tetrahedron formed by sites 2, 4, 5, and 7 (see Fig. 1) and prefers that position by 59 meV over Tr4. In contrast to N, O, and F, C does not have a strong preference for A15 over bcc so that it does not appear to be a β-W former. There is a report to the contrary,[22] but the material might have been contaminated with O and N. N and F show strong similarities with O: N and F prefer the same position and have only slightly weaker β-W forming tendency than O. Beyond about $10^{a}/_{o}$ N or $11^{a}/_{o}$ F β-W is computed to be more stable than bcc-W.

A general analysis for interstitials in tcp phases is presented. It is shown that the simplest representative of the class of tcp structures, the A15 Cr_3Si prototype structure, can have up to three tetrahedral interstices and up to four triangular-base bipyramid interstices. *Ab initio* studies show that a single tetrahedron and a single bipyramid position only are at local minima of the potential energy. C, N, O, and F cannot dissolve substitutionally in W according to *ab initio* results. N, O, and F have a strong preference for the largest bipyramid interstice in the A15 structure in which all nn W atoms are at about equal distance from the interstitial solute. Such regular bipyramid interstices are generally available in tcp phases but not in bcc. As a consequence, N, O, F have a strong preference for β-W. Of order $10^{a}/_{o}$ of these elements dissolved in W is computed to be adequate to stabilize β-W over bcc-W in accord with experimental observations. Ordering of interstitials in β-W might be responsible for the observation of superlattice reflections in transmission electron microscopy.[41,42] The fact that interstitials in β-W need to hop between various tetrahedral and bipyramid positions which are more than 1 eV apart in energy, all but guarantees that activation energies for diffusion in β-W must be higher than in bcc-W. This might explain the apparent stability, or sluggish reaction kinetics, observed in rather defect-free β-W nanowires.[41,43]

TABLE II. Excess enthalpies of C, N, and F in W.

α,p	$H^{\alpha,p}$ eV/cell	$\Delta H_{xs}^{\alpha,p}$ eV/X
bcc $W_{54}C^{(o)}$	−704.959	−7.241
bcc $W_{54}C^{(t)}$	−703.473	−5.755
A15 $W_{48}C_{16}^{(Si)}$	−694.599	−4.900
A15 $W_{64}C^{(Th2)}$	−828.262	−6.665
A15 $W_{64}C^{(Th3)}$	−827.437[a]	−5.840 [a]
A15 $W_{64}C^{(Tr1)}$	−826.454[a]	−4.857 [a]
A15 $W_{64}C^{(Tr4)}$	−828.967	−7.369
bcc $W_{54}N^{(o)}$	−704.683	−6.965
bcc $W_{54}N^{(t)}$	−703.979	−6.261
A15 $W_{48}N_{16}^{(Si)}$	−676.016	−3.739
A15 $W_{64}N^{(Th2)}$	−828.417	−6.819
A15 $W_{64}N^{(Th3)}$	−827.475[a]	−5.878 [a]
A15 $W_{64}N^{(Tr1)}$	−827.066[a]	−5.469 [a]
A15 $W_{64}N^{(Tr4)}$	−829.416	−7.818
bcc $W_{54}F^{(o)}$	−696.250	1.468
bcc $W_{54}F^{(t)}$	−696.864	0.854
A15 $W_{48}F_{16}^{(Si)}$	−603.792	0.775
A15 $W_{64}F^{(Th2)}$	−821.331	0.266
A15 $W_{64}F^{(Th3)}$	−820.733[a]	0.864[a]
A15 $W_{64}F^{(Tr1)}$	−820.034[a]	1.563[a]
A15 $W_{64}F^{(Tr4)}$	−821.472	0.125

[a] Th3 and Tr1 are saddle-point configurations.

M.S. acknowledges support by the Netherlands Institute for Metals Research (www.nimr.nl) in collaboration with the Foundation for Fundamental Research on Matter (FOM) of the Netherlands under Project No. 02EMM032.

---

*m.h.f.sluiter@tudelft.nl

[1] P. Villars, K. Cenzual, J. L. C. Daams, F. Hulliger, T. B. Massalski, H. Okamoto, K. Osaki, A. Prince, and S. Iwata, *Pauling File: Inorganic Materials Database and Design System*, Binaries Edition (ASM International, Metal Park, OH, 2003).
[2] W. G. Burgers and J. A. M. van Liempt, Rev. Trav. Chim. **50**, 1050 (1931).
[3] G. Hägg and N. Schönberg, Acta Crystallogr. **7**, 351 (1954).
[4] K. Kimoto and I. Nishida, J. Phys. Soc. Jpn. **22**, 744 (1967).
[5] J. Forssell and B. Persson, J. Phys. Soc. Jpn. **29**, 1532 (1970).
[6] I. Nishida, T. Sahashi, and K. Kimoto, Thin Solid Films **10**, 265 (1972).
[7] W. B. Blocha, N. T. Gladkich, and I. E. Protsenko, Krist. Tech. **7**, 1201 (1972) in German.
[8] I. Nishida and K. Kimoto, Thin Solid Films **23**, 179 (1974).
[9] Y. Saito, S. Yatsuya, K. Mihama, and R. Uyeda, J. Cryst. Growth **45**, 501 (1978).
[10] Y. Saito, K. Mihama, and R. Uyeda, Jpn. J. Appl. Phys. **19**, 1603 (1980).
[11] M. Gasgnier and L. Névot, Phys. Status Solidi A **66**, 525 (1981).
[12] S. Iwama and K. Hayakawa, Surf. Sci. **156**, 85 (1985).
[13] M. Arita, N. Suzuki, and I. Nishida, Philos. Mag. A **81**, 1597

(2001).

[14] M. H. F. Sluiter, CALPHAD: Comput. Coupling Phase Diagrams Thermochem. **30**, 357 (2006).

[15] M. H. F. Sluiter, Acta Mater. **55**, 3707 (2007).

[16] M. H. F. Sluiter, K. Esfarjani, and Y. Kawazoe, Phys. Rev. Lett. **75**, 3142 (1995).

[17] C. Berne, M. H. F. Sluiter, Y. Kawazoe, T. Hansen, and A. Pasturel, Phys. Rev. B **64**, 144103 (2001).

[18] M. H. F. Sluiter, A. Pasturel, and Y. Kawazoe, Phys. Rev. B **67**, 174203 (2003).

[19] M. H. F. Sluiter, A. Pasturel, and Y. Kawazoe, in *The Science of Complex Alloy Phases*, edited by P. Turchi and T. Massalski (TMS, Warrendale, PA, 2005), p. 409.

[20] M. Arita and I. Nishida, Jpn. J. Appl. Phys. **32**, 1759 (1993).

[21] M. J. O'Keefe, J. T. Grant, and J. S. Solomon, J. Electron. Mater. **24**, 961 (1995).

[22] G. M. Demyashev, R. K. Chuzhko, A. I. Krasovskii, V. P. Kuzmin, M. B. Malandin, Inorg. Mater. **21**, 1007 (1985).

[23] K. K. Lai and H. H. Lamb, Thin Solid Films **370**, 114 (2000).

[24] D. C. Paine, J. C. Bravman, and C. Y. Yang, Appl. Phys. Lett. **50**, 498 (1987).

[25] U. Jansson, Appl. Surf. Sci. **73**, 51 (1993).

[26] C. A. van der Jeugd, G. J. Leusink, G. C. A. M. Janssen, and S. Radelaar, Appl. Phys. Lett. **57**, 354 (1990).

[27] N. Radic, A. Tonejc, J. Ivkov, P. Dubcek, S. Bernstorff, and Z. Medunic, Surf. Coat. Technol. **180-181**, 66 (2004).

[28] Y. G. Shen and Y. W. Mai, J. Mater. Sci. **36**, 93 (2001).

[29] J. P. Perdew and Y. Wang, Phys. Rev. B **45**, 13244 (1992).

[30] G. Kresse and J. Furthmüller, Comput. Mater. Sci. **6**, 15 (1996).

[31] G. Kresse and J. Furthmüller, Phys. Rev. B **54**, 11169 (1996).

[32] P. E. Blöchl, Phys. Rev. B **50**, 17953 (1994).

[33] G. Kresse and D. Joubert, Phys. Rev. B **59**, 1758 (1999).

[34] H. J. Monkhorst and J. D. Pack, Phys. Rev. B **13**, 5188 (1976).

[35] M. Methfessel and A. T. Paxton, Phys. Rev. B **40**, 3616 (1989).

[36] P. E. Blöchl, O. Jepsen, and O. K. Andersen, Phys. Rev. B **49**, 16223 (1994).

[37] The enthalpy of A15 is about 83 meV/atom higher than bcc.

[38] I. A. Weerasekera, S. Ismet Shah, D. V. Baxter, and K. M. Unruh, Appl. Phys. Lett. **64**, 3231 (1994).

[39] M. J. O'Keefe and J. T. Grant, J. Appl. Phys. **79**, 9134 (1996).

[40] Y. G. Shen and Y. W. Mai, Mater. Sci. Eng., A **284**, 176 (2000).

[41] K. L. Klein, S. J. Randolph, J. D. Fowlkes, L. F. Allard, H. M. Meyer III, M. L. Simpson, and P. D. Rack, Nanotechnology **19**, 345705 (2008).

[42] T. Kizuka, T. Sakamoto, and N. Tanaka, J. Cryst. Growth **131**, 439 (1993).

[43] T. Karabacak, P.-I. Wang, G.-C. Wang, and T.-M. Lu, Thin Solid Films **493**, 293 (2005).